

Supporting Information

Seamless Signal Transduction from Three-Dimensional-Cultured Cells to a Superoxide Anions Biosensor via in Situ Self-Assembly of Dipeptide Hydrogel

Meiling Lian,[†] Liang Xu,[†] Xiaowen Zhu,[†] Xu Chen,^{*,†} Wensheng Yang,[†]
and Tie Wang^{*,‡,§}

[†]State Key Laboratory of Chemical Resource Engineering, Beijing University of Chemical Technology, Beijing 100029, China

[‡]Beijing National Laboratory for Molecular Sciences, Key Laboratory of Analytical Chemistry for Living Biosystems, Institute of Chemistry, Chinese Academy of Sciences, Beijing 100190, China

[§]University of Chinese Academy of Sciences, Beijing 100049, China

E-mail: chenxu@mail.buct.edu.cn; wangtie@iccas.ac.cn

Table of Contents

Supplementary Table.....	S3
Supplementary Figures.....	S4-S15
Figure S1 Photograph of the CSH-hydrogel.	S4
Figure S2 AFM image of the CSH-hydrogel	S5
Figure S3 CVs of different modified electrodes	S6

Figure S4 SEM images and corresponding element mapping for hydrogels.....	S7
Figure S5 The activity and leakage of HRP and SOD.....	S8
Figure S6 Cell proliferation assay	S9
Figure S7 CVs of the HRP/Fmoc-FF hydrogel/GCE at different scan rates.	S10
Figure S8 Current-time response of the SH-hydrogel/GCE	S11
Figure S9 Selectivity and stability experiments	S12
Figure S10 The current response at different amount of cells	S13
Figure S11 The current responses at different days	S14
Figure S12 The current responses at different concentration of Zym	S15
Compare the in-situ assembly method and preassembled method	S16
References.....	S17

Table S1. Comparison of the analytical performance of the proposed $O_2^{\cdot-}$ biosensor with other biosensors.

Electrodes	Sensitivity (μA $\mu M^{-1} cm^{-2}$)	LOD (nM)	Linear range (μM)	Ref.
SiO ₂ -Mn ₃ (PO ₄) ₂ /MWCNTs/GCE	1.940	17.5	0.03 - 0.21	1
	1.804		0.15 - 3.6	
Cyt c/NPGM	7.290	0.07		2
Co ₃ (PO ₄) ₂ NRs/GCE	145	2.25	0.00567-5.396	3
Co ₂ P/ZnO@PC/CNTs/GCE	0.328	2160	6.5-4416	4
SOD/porous Pt-Pd/SPCE	1.270	130	16–1536	5
SOD/Pt-Pd/MWCNTs/SPGE	0.601	710	40–1550	6
SOD/NTA/GCE	0.264	21	0.1–100	7
SOD/HRP/PPy/GCE	0.114±0.006		0.01-10	8
SH-hydrogel/GCE	95.28	0.35	0.00105-0.24231	This work
CSH-hydrogel/GCE	85.02	0.34	0.00096-0.18762	This work

NPGM, nanoporous gold mesh; PC, porous carbon polyhedral; NTA, Nitrilotriacetic acid; PPy, polypyrrole.



Figure S1. Photograph of the CSH-hydrogel.

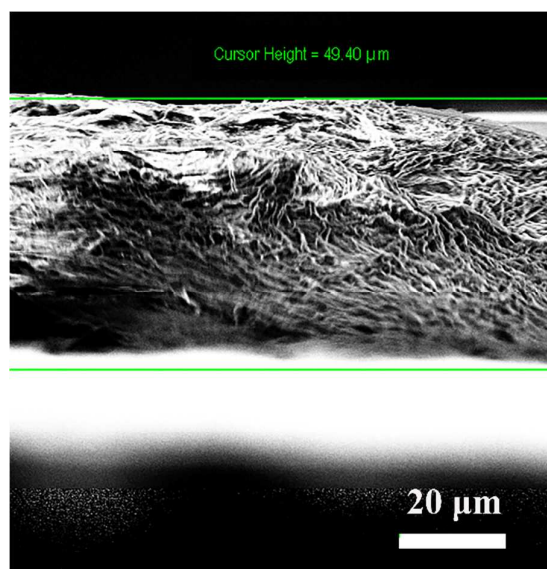


Figure S2. A typical cross-sectional SEM image of the CSH-hydrogel.

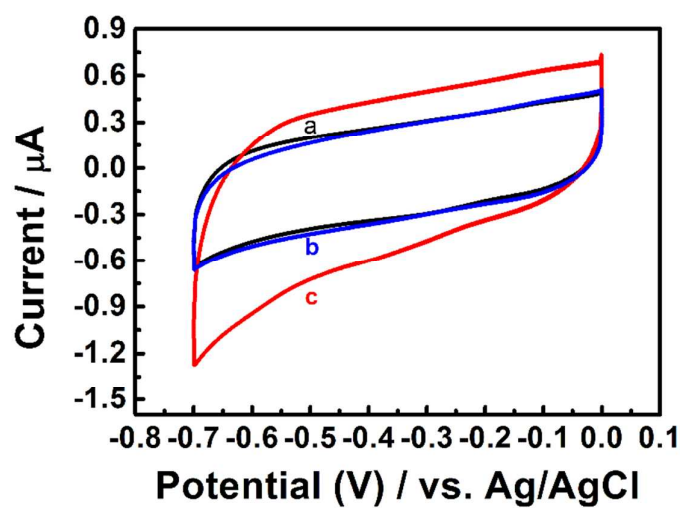


Figure S3. CVs of the (a) SOD/GCE, (b) SOD/HRP/GCE and (c) CS-hydrogel/GCE in 0.1 M PBS (pH 7.0) at a scan rate of 0.1 V s^{-1} .

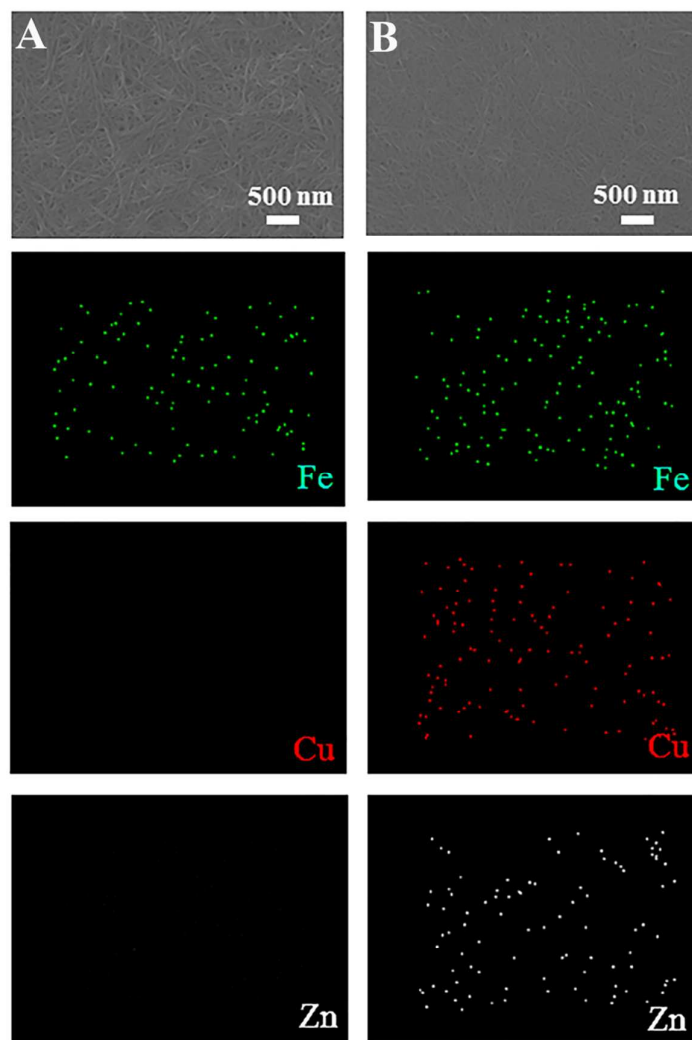


Figure S4. SEM images and corresponding element mapping for (A) H-hydrogel and (B) SH-hydrogel.

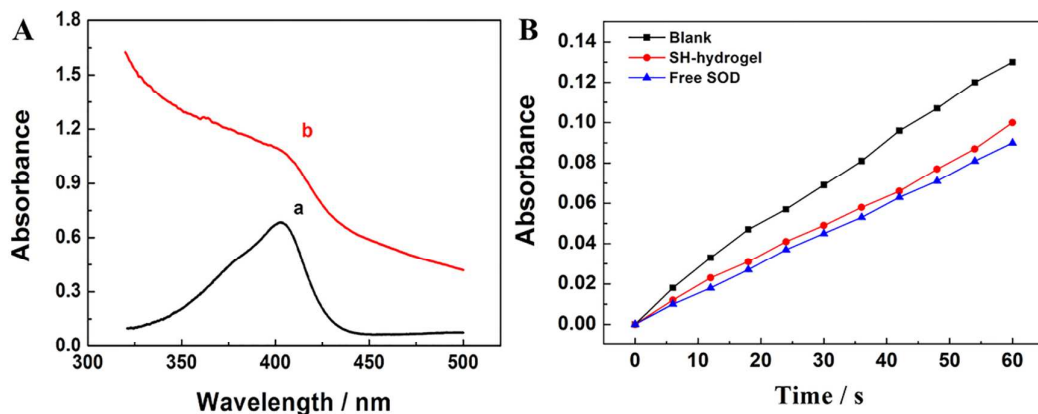


Figure S5. (A) UV-vis spectra of (a) HRP, (b) the SH-hydrogel. (B) The activity of SOD was determined in the system with 10 μ L pyrogallol (50 mM) and 10 μ L SH-hydrogel into the Tris-HCl solution (3 mL, 50 mM, pH=8.2) at 325 nm.

To detect the leakage of the enzymes, deionized water was added to the top surface of the hydrogel, contained in a cuvette, which was collected and analyzed by the UV absorbance of the residual free enzymes. The residual HRP in the supernatant liquid could be quantified by the UV absorbance at 403 nm.⁹ The leakage of SOD was assayed based on the ability of SOD to inhibit the autoxidation of pyrogallol.¹⁰ It can be seen that the relative amounts of HRP and SOD released from the hydrogel were calculated to be approximately 4.2 and 7.1 wt %, respectively.

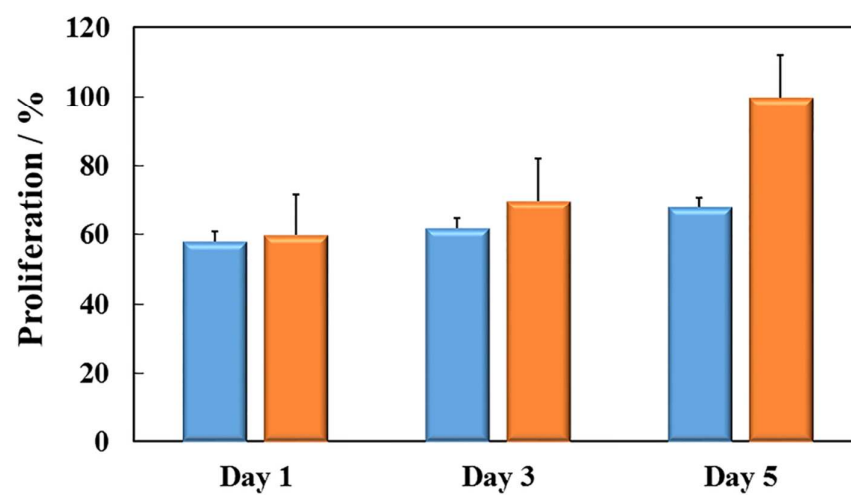


Figure S6. Cell proliferation based on a CCK8 assay within the Fmoc-FF hydrogel (blue), and the tissue culture plastic control (orange).

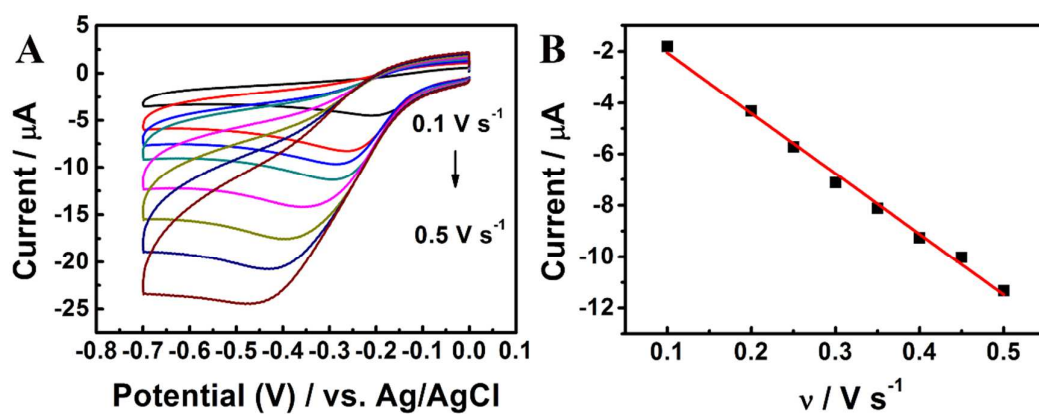


Figure S7. CVs of the (A) CSH-hydrogel/GCE in 0.1 M PBS containing 1 μM H_2O_2 at different scan rates. (B) Relationship between the cathodic peak currents of CSH-hydrogel/GCE and the scan rates.

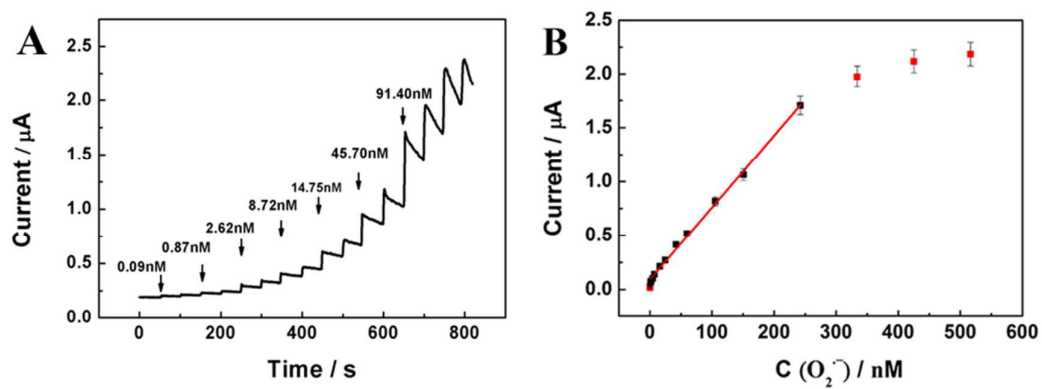


Figure S8. (A) Current-time response of the SH-hydrogel/GCE to the continuous addition of $O_2^{\bullet-}$ in stirred 0.1 M PBS (pH 7.0). (B) Plot of steady-state current vs. $O_2^{\bullet-}$ concentration.

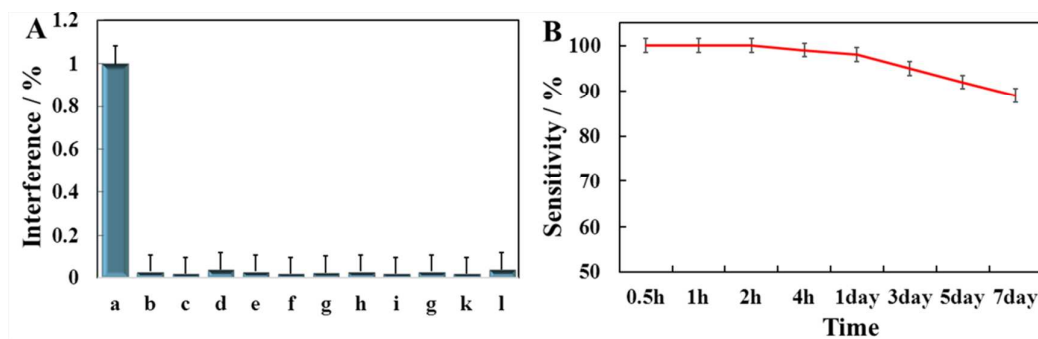


Figure S9. (A) Effects of common interfering species including (a) $\text{O}_2^{\bullet-}$, (b) citric acid, (c) dopamine, (d) ascorbic acid, (e) uric acid, (f) tyrosine, (g) citric acid, (h) glucose, (i) Ca^{2+} , (g) Mg^{2+} , (k) Ni^{2+} , (l) Ag^+ (100 nM for a to l) by using CSH-hydrogel/GCE. (B) Stability test for the CSH-hydrogel/GCE stored at 37 °C in the medium to 100 nM $\text{O}_2^{\bullet-}$ at -0.35 V vs. Ag/AgCl in 0.1 M PBS (pH 7.0).

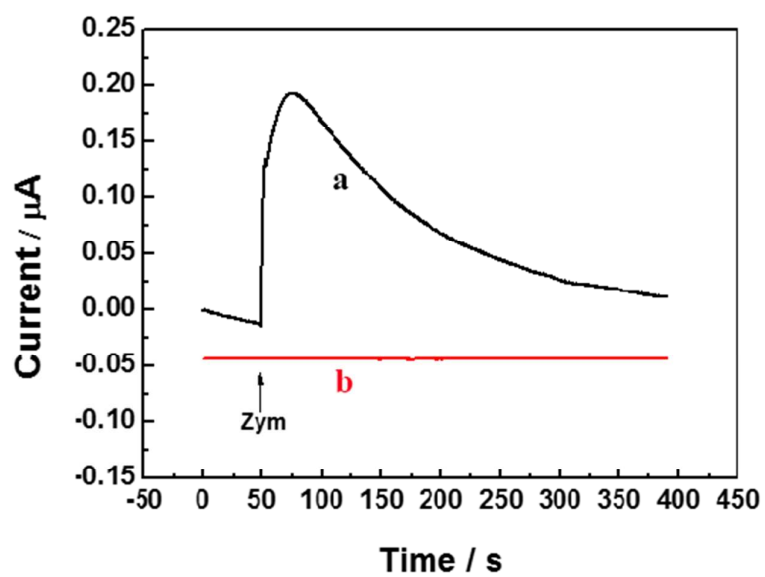


Figure S10. Amperometric responses of CSH-hydrogel/GCE in the presence (a) and absence (b) of HeLa cells (1.0×10^7 cells mL^{-1}) induced by Zym ($30 \mu\text{g mL}^{-1}$) in 0.1 M PBS (pH 7.0) at -0.35 V vs. Ag/AgCl.

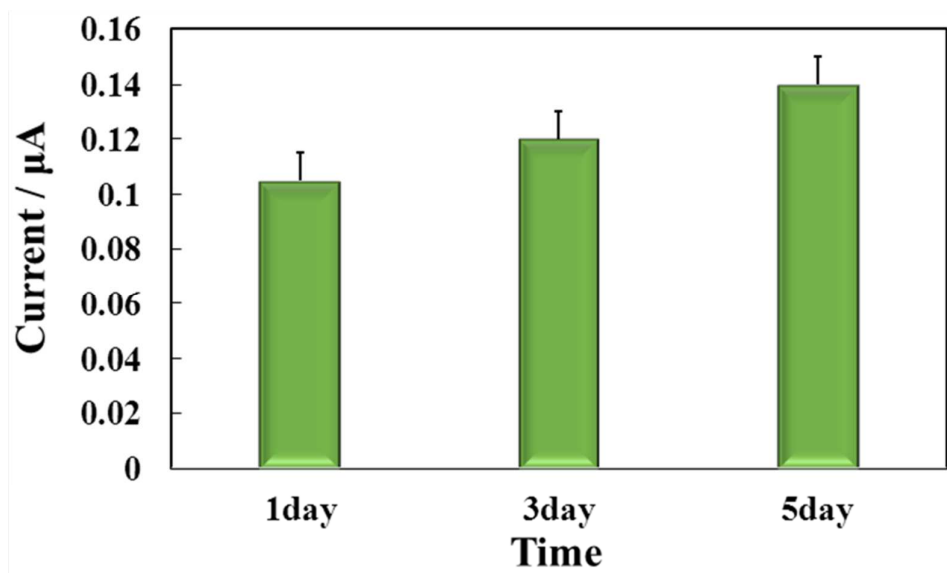


Figure S11. The increase of the peak current obtained at the CSH-hydrogel/GCE induced by Zym ($30 \mu\text{g mL}^{-1}$) at different days.

Previous literature¹¹ has reported the preassembled method in which cells were cultured in the Fmoc diphenylalanine hydrogels. No net proliferation was seen after the first three days of cultivation, while measurable growth was evident after 7 days. In our in suit assembly experiment, spontaneous gel was formed by simply adding a concentrated peptide monomer solution to the cell dispersion. Over the first three days, relatively few growth was detected, while cell viability remained. On the fifth day, the cells have been proliferated. The main reason is that the self-assembly of the hydrogel is accomplished in a cell-containing medium which provides better nutrition for the cells.

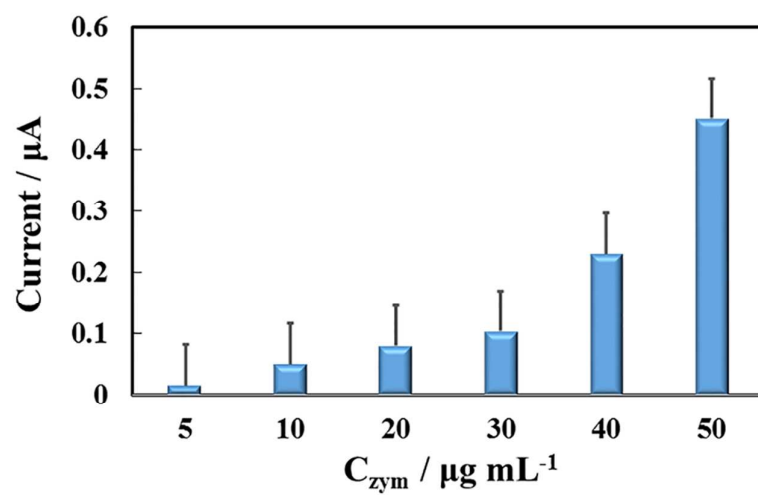


Figure S12. The increase of the peak current obtained at the CSH-hydrogel/GCE induced by different concentration of Zym.

Compared with the preassembled method, in situ assembly method delivers considerably superior detection performance. First, the distance between the enzyme and the cells is different. The in-situ assembly approach will provide more uniform contact of the enzymes and cells than that of the preassembly method, which considerably delivers superior detection performance. Secondly, the assembly conditions are different. According to the literature,¹¹ the use of strong acids and bases in the preassembly method will affect the activity of the enzymes, thereby affecting the sensitivity of ROS detection. For in situ assembly method, enzymes and living cells suspended within the dispersion medium were easily immobilized with addition of the gelling agent, and the relatively high activities of enzymes within the hydrogel were maintained.

REFERENCES

- (1) Shen, X.; Wang, Q.; Liu, Y.; Xue, W.; Ma, L.; Feng, S.; Wan M.; Wang F.; Mao, C. *Sci. Rep.* **2016**, *6*, 28989.
- (2) Sadeghian, R. B.; Han, J.; Ostrovidov, S.; Salehi, S.; Bahraminejad, B.; Ahadian, S., Chen M.; Khademhosseini, A. *Biosens. Bioelectron.* **2017**, *88*, 41–47.
- (3) Wang, M. Q.; Ye, C.; Bao, S. J.; Xu, M. W.; Zhang, Y.; Wang, L., Ma X. Q.; Guo J.; Li, C. M. *Biosens. Bioelectron.* **2017**, *87*, 998–1004.
- (4) Wang, M. Q.; Ye, C.; Bao, S. J.; Zhang, Y.; Xu, M. W.; Li, Z. *Chem. Comm.* **2016**, *52*, 12442–12445.
- (5) Zhu, X.; Liu, T.; Zhao, H.; Shi, L.; Li, X.; Lan, M. *Biosens. Bioelectron.* **2016**, *79*, 449–456.
- (6) Zhu, X.; Niu, X.; Zhao, H.; Tang, J.; Lan, M. *Biosens. Bioelectron.* **2015**, *67*, 79–85.
- (7) Wang, Z.; Liu, D.; Gu, H.; Zhu, A.; Tian, Y.; Shi, G. *Biosens. Bioelectron.* **2013**, *43*, 101–107.
- (8) Lvovich, V.; Scheeline, A. *Anal. Chem.* **1997**, *69*, 454–462.
- (9) Feng, D.; Liu, T. F.; Su, J.; Bosch, M.; Wei, Z.; Wan, W.; Yuan D.; Chen Y, P.; Wang X.; Wang K.; Lian X.; Gu Z. Y.; Park J.; Zou X.; Zhou H. *Nat. Commun.* **2015**, *6*, 5979.
- (10) Wang, X.; Niu, D.; Li, P.; Wu, Q.; Bo, X.; Liu, B.; Bao S.; Su T.; Xu H.; Wang, Q. *ACS Nano*, **2015**, *9*, 5646–5656.
- (11) Jayawarna, V.; Ali, M.; Jowitt, T. A.; Miller, A. F.; Saiani, A.; Gough, J. E.; Ulijn, R. V. *Adv. Mater.* **2006**, *18*, 611–614.